

# Cross-Linker-Free *N*-Isopropylacrylamide Gel Nanospheres

Jun Gao and Barbara J. Frisken\*

Department of Physics, Simon Fraser University,  
Burnaby, British Columbia V5A 1S6, Canada

Received December 10, 2002. In Final Form: March 31, 2003

We have found that the free-radical polymerization of *N*-isopropylacrylamide (NIPAM) in water initiated by potassium persulfate at temperatures well above the phase transition temperature leads to the formation of gel nanospheres instead of linear chains even in the absence of added cross-linker. These particles, with radii of several hundred nanometers, resemble normal NIPAM microgels in every aspect except that they are characterized by lower solid contents and larger swelling ratios than *N,N*-methylene bis(acrylamide) cross-linked microgels synthesized under similar conditions. Without added cross-linker, the formation of gel nanospheres is attributed to self-cross-linking by chain transfer reaction during and after polymerization.

## Introduction

Poly(*N*-isopropylacrylamide) (PNIPAM) has aroused great interest for many years<sup>1</sup> because of its interesting thermal properties; in water, it is characterized by a sharp volume phase transition at a lower critical solution temperature (LCST).<sup>2</sup> By copolymerizing with a divinyl group cross-linker *N,N*-methylene bis(acrylamide) (BIS), this polymer can form a hydrogel, a water-containing polymer chain network. Tanaka's early work on bulk *N*-isopropylacrylamide (NIPAM) hydrogels using simple microscopic observation and subsequent studies has led to a good understanding of the gel phase transition properties.<sup>3</sup> By exploiting the unique thermal properties of NIPAM gels, materials for many interesting applications including controlled drug delivery,<sup>4</sup> artificial muscles,<sup>5</sup> shape memory,<sup>6</sup> sensors,<sup>7</sup> and chromatography<sup>8</sup> have been designed.

In 1986, R. H. Pelton's group first synthesized NIPAM microgels, gel particles with diameters of around 1  $\mu\text{m}$ ,<sup>9</sup> using precipitation polymerization, a technique similar to surfactant-free emulsion polymerization of styrene. In this method, a water solution containing monomer and cross-linker is heated to 70 °C, well above the LCST of PNIPAM, where an initiator is added. As the polymer chains form, they aggregate and are cross-linked into nanoparticles that are stabilized by a combination of electrostatic and steric forces. On cooling below the LCST, the particles do not dissociate into their component polymer chains but exist as stable particles. These particles also show a sharp volume transition and have been used in many applications.<sup>10</sup>

In normal chemical gel formation, a chemical cross-linker is incorporated to create links between polymer

chains. In some cases, cross-linking can also occur without the introduction of a chemical cross-linker, for example, under the influence of irradiation of photoactive comonomers<sup>11</sup> or by  $\gamma$ -irradiation of a linear chain solution.<sup>12</sup> Cross-linking can also occur in the absence of a cross-linker due to chain transfer reaction; recently, gelation in a material related to PNIPAM, poly(*N*-vinylformamide), has been attributed to this process.<sup>13</sup> However, the formation of PNIPAM particles in the absence of added cross-linker has only been mentioned briefly without explanation.<sup>14</sup>

In this work, we describe the synthesis of NIPAM nanospheres without the use of added cross-linker. The formation of the nanospheres appears to be due to the self-cross-linking of polymer chains into a polymer chain network inside each particle and occurs both during and after the polymerization of NIPAM monomer at temperatures much higher than the LCST, where the resultant polymer chains associate into high-density nanoaggregates. Laser light scattering (LLS) is used to characterize the size, molar mass, and solid density of the resultant gel particles. Self-cross-linking is often avoided because it is harmful in the synthesis of linear chain products or reversible gels. However, in this case it can be exploited to synthesize gel particles that are both surfactant- and cross-linker-free and have solid contents as low as 1.3% at 25 °C. This may also lead to a simple way of synthesizing gel particles with a more uniform distribution of cross-linking points than can be obtained using chemical cross-linkers.<sup>11</sup>

## Materials and Method

**Synthesis of Linear Chains and Particles.** NIPAM from Acros Organics (Geel, Belgium) was recrystallized from hexane/acetone solution. Potassium persulfate (KPS) from Aldrich, tetrahydrofuran (THF) from BDH, acetone from Anachemia, and *N,N,N,N*-tetramethyl-ethylene-diamine (TEMED) from Kodak, all analytical grades, were used as received. Fresh deionized water from a Milli-Q Plus water purification system (Millipore, Bedford, with a 0.2  $\mu\text{m}$  filter) was used throughout this work.

(11) Duan Vo, C.; Kuckling, D.; Adler, H. J. P.; Schonhoff, M. *Colloid Polym. Sci.* **2002**, *280*, 400.

(12) Wang, B.; Mukataka, S.; Kodama, M.; Kokufuta, E. *Langmuir* **1997**, *13*, 6108.

(13) Gu, L.; Zhu, S.; Hrymak, A. H.; Pelton, R. H. *Macromol. Rapid Commun.* **2001**, *22*, 212.

(14) McPhee, W.; Tam, K. C.; Pelton, R. H. *J. Colloid Interface Sci.* **1993**, *156*, 24.

\* Corresponding author. E-mail: frisken@sfu.ca.

(1) Schild, H. G. *Prog. Polym. Sci.* **1992**, *17*, 163.

(2) Wu, C. *Polymer* **1998**, *39*, 4609.

(3) Hirose, Y.; Amiya, T.; Hirokawa, Y.; Tanaka, T. *Macromolecules* **1987**, *20*, 1342. Matsuo, E. S.; Tanaka, T. *J. Chem. Phys.* **1988**, *89*, 1695. Li Y.; Tanaka, T. *J. Chem. Phys.* **1989**, *90*, 5161; **1990**, *92*, 1365.

(4) Hoffman, A. S.; Afrassibi, A.; Dong, L. C. *J. Controlled Release* **1986**, *4*, 213. Hoffman, A. S. *J. Controlled Release* **1987**, *6*, 297.

(5) Osada, Y.; Ross-Murphy, S. B. *Sci. Am.* **1993**, *268*, 82.

(6) Hu, Z.; Zhang, X.; Li, Y. *Science* **1995**, *269*, 525.

(7) Weissman, J. M.; Sunkara, H. B.; Tse, A. S.; Asher, S. A. *Science* **1996**, *274*, 959. Holtz, J. H.; Asher, S. A. *Nature* **1997**, *389*, 829.

(8) Kikuchi, A.; Okano, T. *Prog. Polym. Sci.* **2002**, *27*, 1165.

(9) Pelton, R. H.; Chibante, P. *Colloids Surf.* **1986**, *20*, 247.

(10) Pelton, R. H. *Adv. Colloid Interface Sci.* **2000**, *85*, 1.

**Table 1. Summary of Synthesis Conditions for PNIPAM Particles**

batch no.	synthesis		concentration (100 g initial solution)	
	$T$ (°C)	$t$ (h)	$W_{\text{NIPAM}}$ (g)	$W_{\text{KPS}}$ (mg)
009	$70 \pm 1$	4.0	1.00	40
058	$70 \pm 1$	4.0	1.00	5

To synthesize linear PNIPAM chains, a 20 mL solution containing 1.51 g of NIPAM monomer and 9.65 mg of KPS initiator was first nitrogen purged in a vial for 15 min. After introducing 60  $\mu\text{L}$  of TEMED, the sealed vial was immersed in ice water. Polymer chains formed by free radical polymerization in a few minutes as observed by passing a He–Ne laser beam through the sample. After 1 day, the resultant chains were purified by precipitation followed by washing in an acetone/water mixture three times and drying in a fume hood and vacuum oven.

To synthesize NIPAM particles, the NIPAM solution was stirred under a nitrogen atmosphere in a 150 mL reactor for  $\sim 30$  min and heated to 70 °C, well above the LCST for PNIPAM, using a digital heating plate and a water bath covered with a thin layer of paraffin oil. KPS water solution was added to the reactor to initiate polymerization. The reaction system was stirred at the incubation temperature for a time sufficient to ensure that all the monomer was exhausted. The final reaction dispersion was characterized after it had been cooled to room temperature. Table 1 contains details of the reaction conditions used for the different samples, batches 009 and 058, used in this study.

**Laser Light Scattering.** The apparatus used for light scattering measurements was an ALV DLS/SLS-5000 spectrometer/goniometer equipped with an ALV-5000 digital time correlator and a helium–neon laser.

We used static light scattering (SLS) to measure the weight-average molar mass  $M_w$  and the z-average root-mean-square radius of gyration  $R_g$ . For small particles, we used a standard Zimm plot analysis to find  $M_w$  and  $R_g$  of the particles from the Rayleigh ratio  $R_{90}(q)$  determined from the time-averaged scattered intensity<sup>15</sup>

$$\frac{KC}{R_{90}(q)} \approx \frac{1}{M_w} \left( 1 + \frac{1}{3} R_g^2 q^2 \right) + 2A_2 C \quad (1)$$

where  $K = 4\pi^2 n^2 (dn/dc)^2 / (N_A \lambda_0^4)$ ,  $q = (4\pi n / \lambda_0) \sin(\theta/2)$  is the magnitude of the scattering wave vector and  $A_2$  is the second virial coefficient, with  $N_A$ ,  $n$ ,  $C$ ,  $\lambda_0$ , and  $\theta$  being Avogadro's constant, the solvent refractive index, the solid concentration (g/mL), the light wavelength in a vacuum, and the scattering angle, respectively. For PNIPAM, values of 0.167 and 0.174 mL/g at 25 and 40 °C, respectively, were used for  $dn/dc$ .<sup>16</sup> For larger particles, we fit the data to a form

$$\frac{KC}{R_{90}(q, R)} = \frac{1}{M_w P(q, R)} \quad (2)$$

where  $P(q, R) = (3/(q^3 R^3)) (\sin(qR) - qR \cos(qR))^2$  is the form factor for uniform spheres with radius  $R$ , to determine  $M_w$  and  $R$ . We used dynamic light scattering (DLS) to measure the time correlation function of the scattered intensity  $g^{(2)}(\tau)$  as a function of the decay time  $\tau$ . The hydrodynamic radius  $R_h$  and polydispersity of the samples were determined from analysis of  $g^{(2)}(\tau)$  using either CONTIN<sup>17</sup> or a moments-based analysis.<sup>18</sup>

**<sup>13</sup>C NMR.** Solid <sup>13</sup>C analysis was conducted using a domestic solid-state NMR instrument. <sup>13</sup>C NMR spectra were obtained at 37.55 MHz at an ambient temperature of  $24 \pm 1$  °C. Proton–carbon Hartmann–Hahn cross-polarization was used, with matched reference fields of 48 kHz; the same field strength was used for proton decoupling during data acquisition. Magic angle spinning was used, at speeds of 2400 or 2500 Hz.

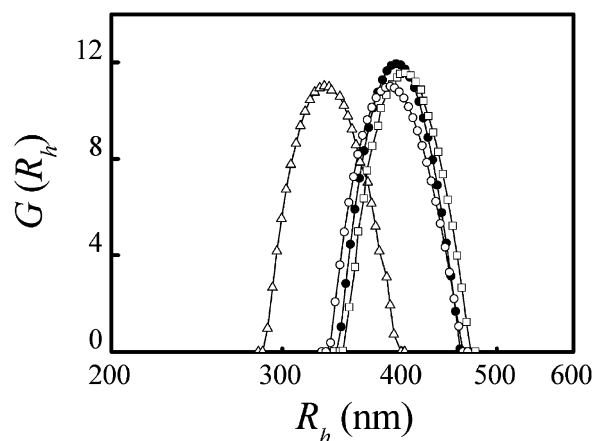


**Figure 1.** Normalized hydrodynamic radius distribution of NIPAM gel nanospheres (batch 009) at 25 °C as produced in water (solid circles,  $C = 2.15 \times 10^{-4}$  g/mL) and after being dried and then redispersed in water (open circles,  $C = 5.39 \times 10^{-5}$  g/mL), acetone (triangles,  $C = 1.92 \times 10^{-4}$  g/mL), and THF (squares,  $C = 2.59 \times 10^{-4}$  g/mL), as measured by DLS at a scattering angle of 30°. The particles are slightly smaller in acetone than in water or THF. The distributions have standard deviations of about 10%.

## Results and Discussion

Under standard conditions for the synthesis of NIPAM gel spheres (except for the absence of cross-linker), the solution became a blue dispersion, indicating small particles of a few tens of nanometers, within 2 min of introducing the initiator, and then a white dispersion, indicating larger particles, within another couple of minutes. After polymerization for 4 h, no dissociation of these aggregates was observed even after incubating the dispersion at room temperature for 1 year or in a refrigerator (2–4 °C) for 1 day. Concentrating the resultant turbid dispersions led to colored and more transparent dispersions, which is the typical optical phenomenon of closely packed narrowly distributed gel nanospheres.<sup>19</sup>

Characterization of these particles by DLS revealed narrow particle size distributions with average hydrodynamic radii ( $R_h$ ) of several hundred nanometers. Figure 1 shows the particle size distribution measured at 25 °C for a dilute water dispersion of particles of batch 009 (solid circles); the sample has an average hydrodynamic radius of 390 nm and a relative standard deviation of about 10%. To test the stability of the particles, the water was evaporated from the original dispersion and dry pieces of the sample were redispersed in different solvents. In THF and acetone, the solid pieces swelled and redispersed thoroughly with gentle vortexing in roughly 10 and 30 min, respectively. In water, it took hours to achieve similar uniformity. The size distributions for these dispersions have shapes and relative standard deviations that are consistent with those of the original dispersion with values for the  $\langle R_h \rangle$  of 360 nm in acetone (triangles), 390 nm in water (open circles), and 405 nm in THF (squares) indicating the affinity of the solvents for the particles. Standard Zimm plot analysis of the SLS data for samples made from the original water dispersion as shown in Figure 2 reveals a  $M_w$  of  $2.0 \times 10^9$  g/mol and a  $R_g \sim \langle R_h \rangle$ . The light scattering results for this sample are summarized in Table 2.

Two models of the structure of the resultant nanoparticles can be imagined to occur under conditions of random free radical polymerization; these are shown in Figure 3.

(15) Zimm, B. H. *J. Chem. Phys.* **1948**, *16*, 1099.

(16) Gao, J.; Wu, C. *Macromolecules* **1997**, *30*, 6873.

(17) Provencher, S. W. *Makromol. Chem.* **1979**, *180*, 201.

(18) Chu, B. *Laser Light Scattering*; Academic Press: Boston, 1991.

(19) Gao, J.; Hu, Z. *Langmuir* **2002**, *18*, 1360.

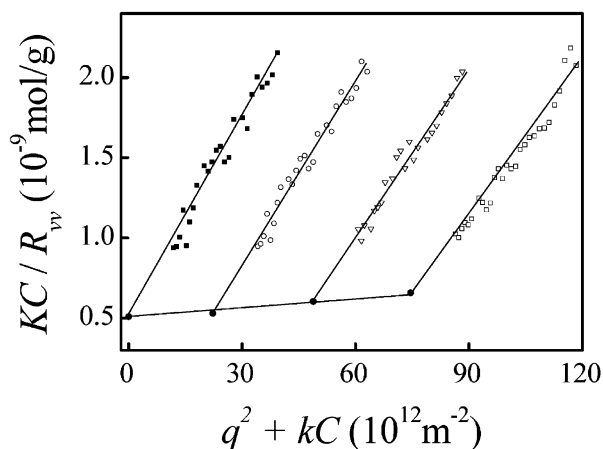


**Figure 2.** Zimm plot of SLS data for NIPAM gel nanospheres (batch 009) dispersed in water at 25 °C at concentrations of  $6.41 \times 10^{-5}$  g/mL (circles),  $1.41 \times 10^{-4}$  g/mL (anti-triangles), and  $2.15 \times 10^{-4}$  g/mL (open squares). The data were measured at scattering angles between 12 and 28°. Solid squares and circles are the results of extrapolating the data to zero concentration and zero angle, respectively.

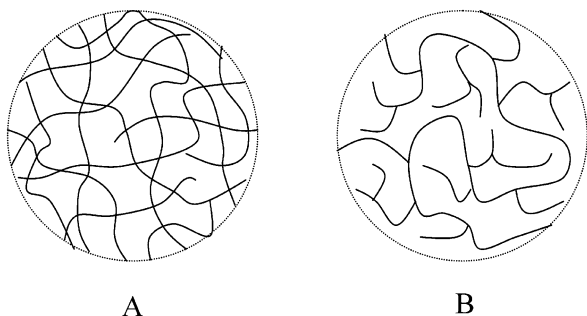


**Figure 3.** Sketch of two possible structures of the resultant nanoparticles: (A) cross-linked networks and (B) hyperbranched chains.

**Table 2. Summary of LLS Results for PNIPAM Particles at 25 °C in Water**

batch no.	$\langle R_h \rangle$ (nm)	$R_g$ (nm)	$M_w$ (g/mol)	$R_g/\langle R_h \rangle$	$\rho$ (g/cm <sup>3</sup> )
009	390	400	$2.0 \times 10^9$	1.0	0.013
058	326	330	$3.7 \times 10^9$	1.0	0.042

Particles having a network structure as shown in Figure 3A are formed by cross-linking between polymer chains. Particles having a branched structure as sketched in Figure 3B are, in contrast, formed by hyperbranching of a single polymer chain.

While these two structures are very similar, it is possible to confirm that the particles are a result of self-cross-linking rather than hyperbranching. The large values for the size and molar mass of these particles obtained from light scattering, while not conclusive, are a good indication that the products of this reaction are cross-linked particles rather than hyperbranched chains. The high stability of the particles in different solvents is also a good indication of the formation of cross-linked structure rather than pure branching structure.

As a further test, we checked whether we could form particles from linear PNIPAM chains in the presence of only an initiator. Chains incubated at low temperature are stable indefinitely, but we found that a transparent solution of linear chains consisting of 1 wt % of PNIPAM and 420 ppm KPS incubated at 70 °C became white and turbid, indicating chain aggregation. After incubation for 4 h in a nitrogen atmosphere, cooling the dispersion to

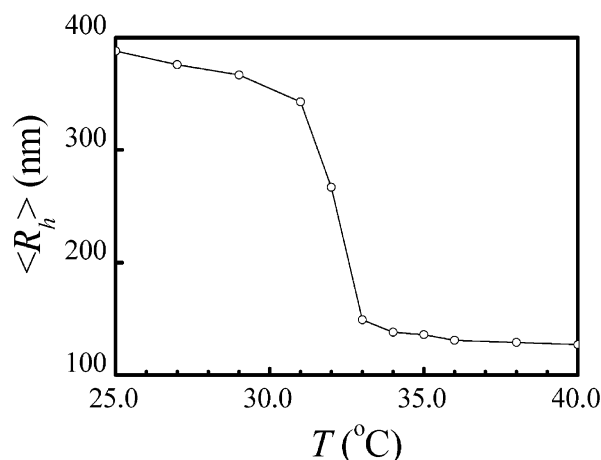


**Figure 4.** The temperature dependence of the hydrodynamic radius of NIPAM gel nanospheres (batch 009) in water, measured at a sample concentration of  $2.15 \times 10^{-4}$  g/mL and a scattering angle of 30°. A curve has been drawn through the data as a guide to the eye. The hydrodynamic radius decreases by a factor of 2.9 on heating.

room temperature resulted in a viscoelastic dispersion indicating that permanent cross-linking between the chains had occurred. Furthermore, we found that incubation of more dilute PNIPAM/KPS solutions at 70 °C resulted in colloidal solutions of particles with  $\langle R_h \rangle \sim 200$  nm and  $M_w \sim 500$  times larger than that of the linear chains before incubation.

Other aspects of these particles can be compared to those of BIS-cross-linked NIPAM nanospheres. The average solid density  $\rho$  for the particles was calculated from the simple relation  $M_w = (4/3)\pi\langle R_h \rangle^3\rho N_A$  because of the narrowness of the size distribution. We found that particles from batches 009 and 058 had solid contents of only 0.013 and 0.042 g/cm<sup>3</sup> at 25 °C, respectively, comparable to values found for gel nanospheres made in the presence of a small amount of cross-linker.<sup>19</sup> The temperature dependence of the average particle size is shown in Figure 4 for a sample from batch 009 heated from 25 to 40 °C. The size of the particles equilibrated within the time required to change the temperature of the sample bath. A sharp decrease in particle size was observed between 32 and 33 °C, consistent with the behavior of PNIPAM gel particles which show a distinct shrinking over this same narrow temperature range.<sup>2</sup> Repeated temperature cycling between 25 and 40 °C led to reproducible data, and the molar mass of the particles did not change during this transition. The decrease in particle size, as measured by the ratio  $\langle R_h \rangle_{25^\circ\text{C}}/\langle R_h \rangle_{40^\circ\text{C}}$ , was 2.9 over this temperature range, resulting in a decrease in the particle volume and an increase in the particle density by a factor of 25. This is slightly larger than usually found for BIS-cross-linked NIPAM microgels<sup>14</sup> but is consistent with a low level of cross-linking. We would expect the swelling at low temperature to be much larger for a hyperbranched polymer chain because in that case there would be no constraining force equivalent to the elastic force in a gel system to constrain its stretch.

Details of the structure of the particles can be inferred by comparing the results of static light scattering, which measures particle size based on their refractive index profiles, and dynamic light scattering, which measures particle size based on their hydrodynamic size. For this sample, the ratio of  $R_g/\langle R_h \rangle$  was measured to be 1.0 at 25 °C and 0.71 at 40 °C, consistent with ratios found for PNIPAM gel spheres. The theoretical values of  $R_g/\langle R_h \rangle$  are 0.77 for uniform spheres and 1.5 or 1.78 for Gaussian

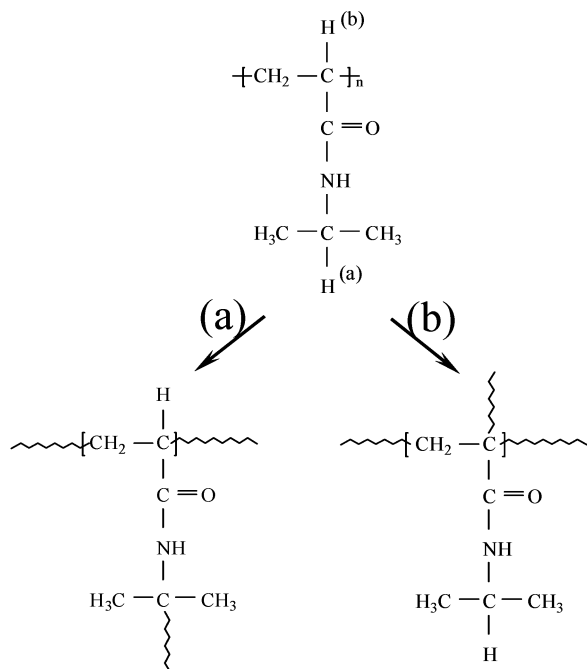


**Figure 5.** Possible positions on a PNIPAM chain for formation of *tert*-C free radicals and resultant structures: (a) the hydrogen atom of the *tert*-C on the pendant isopropyl group or (b) the hydrogen atom on the *tert*-C of the main chain backbone.

chains under theta or good solvent conditions, respectively.<sup>20</sup> Values for these particles, as well as for BIS-cross-linked particles, are consistent with those for uniform spheres.

Since no chemical cross-linker was added, we attribute the formation of stable nanospheres to the self-cross-linking of PNIPAM chains by chain transfer reaction. Figure 5 shows the structure of PNIPAM and the two most probable sites for chain transfer: (a) the hydrogen atom on the *tert*-C of the pendent isopropyl group and (b) the hydrogen atom on the *tert*-C of the main chain backbone. These hydrogen atoms are both active and are likely to be attacked by free radicals, forming *tert*-C free radicals that are stabilized by conjugating with adjacent groups. In either case, the *tert*-C free radical may react further with a vinyl group or with another *tert*-C active H on an adjacent PNIPAM chain to continue the chain reaction, or may be terminated with an oligomer or a macromolecular free radical; all of these possibilities result in potential cross-linking points as shown in routes a and b in Figure 5. The tendency of forming *tert*-C free radicals resulting in branched polymers was first reported many years ago,<sup>21</sup> but chain transfer from the pendent groups has not been extensively reported.<sup>13</sup> Route b may be preferred in PNIPAM because the *tert*-C free radical on the pendent isopropyl group is likely to be further stabilized by the two adjacent methyl groups and has less spatial barrier to propagation or termination than the *tert*-C free radical on the backbone; further investigation is necessary to confirm this speculation.

We attempted to use <sup>13</sup>C NMR as an analytical tool to confirm the existence of cross-linking points. We performed solid <sup>13</sup>C NMR experiments for both spheres from batch 058 and linear PNIPAM chains. The <sup>13</sup>C NMR spectra are shown in Figure 6. Both spectra show three major peaks;

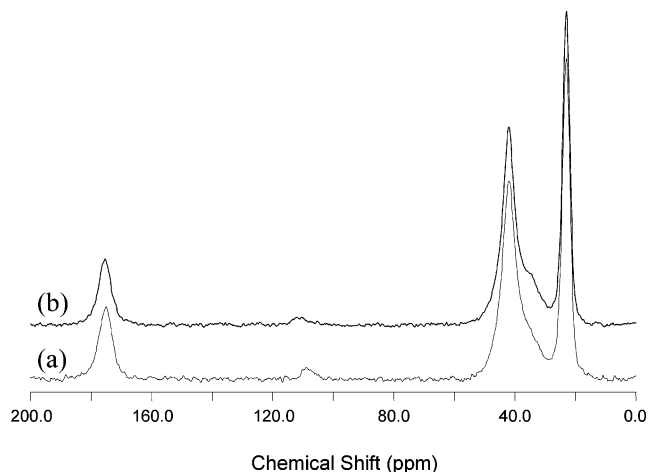


**Figure 6.** <sup>13</sup>C NMR spectra for (a) linear PNIPAM chains and (b) self-cross-linked NIPAM gel nanospheres (batch 058).

the peaks at chemical shifts of 175, 23, and 42 ppm represent the carbon atoms in the carbonyl groups, the carbon atoms in the methyl groups, and the remaining *tert* or secondary carbon atoms, respectively.<sup>22</sup> The small features near 110 ppm are spinning sidebands of the carbonyl peak at 175 ppm. The main difference between the spectra for the linear chains (Figure 6a) and the particles (Figure 6b) is a slight increase in the signal at a chemical shift of 35 ppm for the dried sphere sample. Unfortunately, although this does represent a real change in the spectrum, it is not possible to say what this increase is due to at this time. In general, we expect the difference between the spectra for the linear chain and the particles to be very small due to the fact that only a small fraction of the chains are cross-linked making identification of the cross-linking points by this method difficult.

The kinetics of self-cross-linking was investigated under standard reaction conditions except that the initial  $C_{KPS}$  was decreased from 400 to 50 mg/L in order to get denser and smaller gel spheres that could be more easily characterized by LLS. Figure 7 shows LLS results at 25 °C for samples drawn from batch 058 at different times during the reaction. For these measurements, only one dilute sample with a concentration of  $\sim 10^{-5}$  g/mL was used to obtain  $M_w$  and  $R_g$  for each reaction time. Since the samples are so dilute and  $A_2$  is so small for PNIPAM in water,<sup>19</sup> the difference between  $M_w$  found using only one sample and a group of samples is negligible. During the first half-hour of the reaction,  $\langle R_h \rangle$ ,  $M_w$ , and  $\rho$  increased quickly; subsequently the rate of increase for  $M_w$  and  $\rho$  slowed gradually while  $\langle R_h \rangle$  started to decrease. After about 2 h,  $\langle R_h \rangle$ ,  $M_w$ , and  $\rho$  remained basically unchanged. The existence of stable particles even 10 min into the reaction implies that interchain cross-linking begins immediately during polymerization. The gradual shrinking and related density increase of the particles that occurs after 30 min show that self-cross-linking continues after all of the monomer has been depleted.<sup>10</sup> The light scattering results for the final sample are summarized in Table 2.

Self-cross-linking was further investigated in a KPS-initiated redox system. We added 0.2 mL of TEMED to a standard batch [ $T_{syn} = 70$  °C,  $C_{NIPAM} = 1$  wt %, and  $C_{KPS} = 0.04$  wt %] immediately before adding KPS. TEMED accelerates the decomposition of KPS. Interestingly, only

(20) Burchard, W.; Schmidt, M.; Stockmayer, W. H. *Macromolecules* **1980**, *13*, 1265.

(21) Flory, P. J. *Principles of Polymer Chemistry*; Cornell University Press: New York, 1953.

(22) Kalinowski, H.; Berger, S.; Braun, S. *Carbon-13 NMR Spectroscopy*; John Wiley & Sons: New York, 1984.

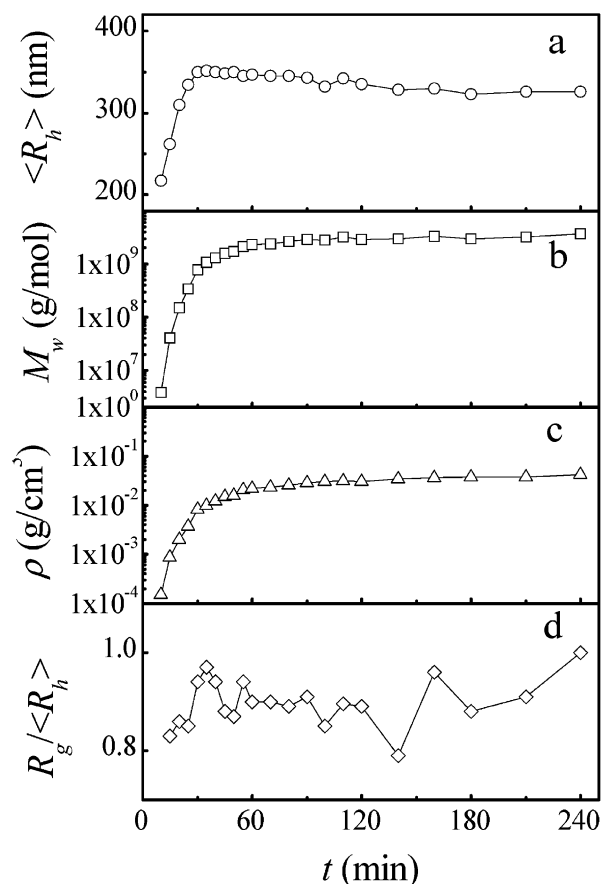


**Figure 7.** (a)  $\langle R_h \rangle$ , (b)  $M_w$ , (c)  $\rho$ , and (d)  $\langle R_h \rangle_{25^\circ\text{C}} / \langle R_h \rangle_{40^\circ\text{C}}$  as a function of the reaction time at a constant initial  $C_{\text{NIPAM}}$  of 10 g/L, a constant initial  $C_{\text{KPS}}$  of 50 mg/L, and a constant  $T_{\text{syn}}$  of 70 °C. Light scattering measurements were made on samples with concentrations  $C \sim 10^{-5}$  g/mL at 25 °C.

a solution of linear chains with  $M_w$  of  $\sim 1.0 \times 10^6$  g/mol was obtained. Several reasons for no discernible self-cross-linking can be considered. One is that chain transfer as required for self-cross-linking is prevented in the presence of TEMED. Alternatively, TEMED may create so many free radicals that the resultant polymer chains are too hydrophilic for efficient cross-linking to occur.

## Conclusions

Free-radical polymerization of NIPAM in water initiated by KPS in the absence of added cross-linker can lead to the formation of stable nanospheres instead of linear chains if the solution is incubated at temperatures well above the LCST of PNIPAM. The resultant particles have molar masses as high as  $10^9$  g/mol, narrow particle size distributions, and solid densities comparable to those observed in BIS-cross-linked gel nanospheres. Formation of particles was also observed in dispersions of linear PNIPAM chain aggregates incubated under similar conditions. The formation of the particles is attributed to interchain self-cross-linking through chain transfer reaction both during and after polymerization. The observation of particle formation due to self-cross-linking during the free radical polymerization of NIPAM at reaction temperatures much higher than the LCST is quite reasonable. At such high temperatures, the resultant polymer chains associate into compact nanoaggregates; this enables the interchain cross-linking in the presence of free radicals especially before the monomer is depleted. The influence of reaction temperature and initial monomer and initiator concentrations on the mass, size, and density of the gel particles has also been investigated and will be summarized in a separate article.<sup>23</sup>

One implication of this study is that intrinsic self-cross-linking is always present if the local solid density becomes high enough and should not be neglected even when some cross-linker is used. It may be necessary to avoid this process during the synthesis of polymer chains or degradable gel networks, but it may be exploited to synthesize gel spheres from collapsed chain aggregates.

**Acknowledgment.** We acknowledge Professor Ian D. Gay for his help with the solid  $^{13}\text{C}$  NMR measurements. Jun Gao expresses his thanks to Drs. Yunsong Yang and Xiaohui Wang for helpful discussions and Professor A. S. Tracey for NMR consultation. This work was supported by the Natural Science and Engineering Research Council of Canada.

LA0269762

(23) Gao, J.; Frisken, B. J. *Langmuir* **2003**, *19*, 5217.